JPET Fast Forward. Published on February 14, 2020 as DOI: 10.1124/jpet.119.262790
This article has not been copyedited and formatted. The final version may differ from this version.

Distinct regulation of sigma-1 receptor multimerization by its agonists and antagonists in transfected cells and rat liver membranes

Weimin Conrad Hong

Department of Pharmaceutical Sciences, Butler University, Indianapolis, IN 46208

JPET Fast Forward. Published on February 14, 2020 as DOI: 10.1124/jpet.119.262790
This article has not been copyedited and formatted. The final version may differ from this version.

a) Running title: *Regulation of σ_1R multimerization by ligands*

b) Corresponding author:

Weimin Conrad Hong Ph.D.,

Department of Pharmaceutical Sciences, Butler University, PB351,

4600 Sunset Avenue, Indianapolis, IN 46208

Email: chong@butler.edu

Phone: 317-940-9580

Fax: 317-940-6172

c) Text pages:

Figures:	8	
Tables:	1	
References:	62	
Words in Abstract:	249	(250 max)
Words in Introduction:	750	(750 max)
Words in Discussion:	1479	(1500 max)

d) Nonstandard abbreviations:

ANOVA: analysis of variance

BD1008: *N*-[2-(3,4-dichlorophenyl)ethyl]-*N*-methyl-2-(1-pyrrolidinyl)ethylamine dihydrobromide

BD1047: *N*-[2-(3,4-dichlorophenyl)ethyl]-*N*-methyl-2-(dimethylamino)ethylamine dihydrobromide

BD1063: 1-[2-(3,4-dichlorophenyl)ethyl]-4-methylpiperazine dihydrochloride

BRET: Bioluminescence resonance energy transfer

CM304: 3-(2-(azepan-1-yl)ethyl)-6-(3-fluoropropyl)-1,3-benzothiazol-2-one hydrochloride

DSP: dithiobis(succinimidyl propionate)

DTG: 1,3-di-*o*-tolylguanidine

FRET: Förster resonance energy transfer

GDN: glyco-diosgenin

HEK293: human embryonic kidney 293

kD: kilodalton

MW: molecular weight

NE-100: 4-methoxy-3-(2-phenylethoxy)-N,N-dipropylbenzeneethanamine monohydrochloride

PAGE: polyacrylamide gel electrophoresis

PBS: phosphate-buffered saline

PBSCM: PBS with $CaCl_2$ and $MgCl_2$

(+)Pent: (+)-pentazocine

PFO: perfluorooctanoic acid

PRE-084: 2-(4-morpholinethyl) 1-phenylcyclohexanecarboxylate hydrochloride

SEM: standard error of mean

SLS: sodium lauroyl sarcosinate

(+)SKF 10047: (+) *N*-allylnormetazocine (NANM) hydrochloride

TCEP: tris(2-carboxyethyl)phosphine

JPET Fast Forward. Published on February 14, 2020 as DOI: 10.1124/jpet.119.262790
This article has not been copyedited and formatted. The final version may differ from this version.

TM: transmembrane domain

σ_1R: sigma$_1$ receptor

FH-σ_1R: sigma$_1$ receptor with N-terminal Flag and 2xHis$_8$ tags

e) Recommended section assignment: Cellular and Molecular

Abstract

Extensive studies have shown that the sigma-1 receptor (σ_1R) interacts with and modulates the activity of multiple proteins with important biological functions. Recent crystal structures of σ_1R as a homo-trimer differ from a dimer-tetramer model postulated earlier. It remains inconclusive whether ligand binding regulates σ_1R oligomerization. Here novel non-denaturing gel methods and mutational analysis were used to examine σ_1R oligomerization. In transfected cells σ_1R exhibited as multimers, dimers and monomers. Overall σ_1R agonists decreased, whereas σ_1R antagonists increased σ_1R multimers, suggesting that agonists and antagonists differentially affect the stability of σ_1R multimers. Endogenous σ_1R in rat liver membranes also showed similar regulation of oligomerization as in cells. Mutations at key residues lining the trimerization interface (Arg119, Asp195, Phe191, Trp136, and Gly91) abolished multimerization without disrupting dimerization. Intriguingly, truncation of the N-terminus reduced σ_1R to apparent monomer. These results demonstrate that multiple domains play crucial roles in coordinating high-order quaternary organization of σ_1R. The E102Q σ_1R mutant implicated in juvenile amyotrophic lateral sclerosis formed dimers only, suggesting that dysregulation of σ_1R multimeric assembly may impair its function. Interestingly, oligomerization of σ_1R was pH dependent and correlated with changes in [^{3}H](+)-pentazocine binding affinity and B_{max}. Combined with mutational analysis, it is reasoned that σ_1R multimers possess high-affinity and high-capacity [^{3}H](+)-pentazocine binding, whereas monomers likely lack binding. These results suggest that σ_1R may exist in interconvertible oligomeric states in a dynamic equilibrium. Further exploration of ligand-regulated σ_1R multimerization may provide novel approaches to modulate the function of σ_1R and its interacting proteins.

JPET Fast Forward. Published on February 14, 2020 as DOI: 10.1124/jpet.119.262790
This article has not been copyedited and formatted. The final version may differ from this version.

Significance statement

The σ_1R modulates the activities of various partner proteins. Recently crystal structures of σ_1R were elucidated as homotrimers. This study used novel non-denaturing gel methods to examine σ_1R oligomerization in transfected cells and rat liver membranes. Overall agonist binding decreased whereas antagonist binding increased σ_1R multimers, which comprised trimers and larger units. σ_1R multimers were shown to bind [^{3}H](+)-pentazocine with high-affinity and high-capacity. Further, mutational analysis revealed a crucial role of its N-terminal domain in σ_1R multimerization.

Introduction

The sigma receptor (σR) was named after the distinct behavioral signs induced by SKF10047 (N-allylnormetazocine) in a chronic spinal dog preparation (Martin et al., 1976). However, molecular cloning identified a 25-kD membrane protein as the sigma-1 receptor (σ_1R) (Hanner et al., 1996; Jbilo et al., 1997). Its sequence is highly conserved in evolution, but distinct from opioid receptors as originally proposed. Multiple alternative splice variants of σ_1R have been characterized (Pan et al., 2017), including an isoform lacking exon 3 (ΔE3) which encodes amino acids (aa) 119–149 (Ganapathy et al., 1999).

Extensive studies have shown that σ_1R can interact with and modulate the activity of a plethora of partner proteins, including channels, receptors, and transporters (Hayashi and Su, 2001; Aydar et al., 2002; Hayashi and Su, 2007; Wu and Bowen, 2008; Carnally et al., 2010; Kim et al., 2010; Navarro et al., 2010; Balasuriya et al., 2012; Kourrich et al., 2013; Srivats et al., 2016; Hong et al., 2017; Sambo et al., 2017; Thomas et al., 2017; Schmidt and Kruse, 2019) that play important roles in cellular homeostasis and neuronal signaling. The majority of σ_1R protein is located in endoplasmic reticulum, particularly mitochondria-associated ER membranes (Hayashi and Su, 2007), which are critical sites to modulate energy balance, calcium regulation, and stress response. Several σ_1R mutations have recently been implicated in juvenile amyotrophic lateral sclerosis (ALS) and distal hereditary motor neuropathies. Molecular mechanisms underlying such motor neuron deficits have been studied intensively, and aberrant σ_1R expression and function appear to be crucial in these conditions (Al-Saif et al., 2011; Bernard-Marissal et al., 2015; Li et al., 2015; Gregianin et al., 2016; Watanabe et al., 2016; Dreser et al., 2017).

Many clinical drugs and synthetic compounds with diverse structures exhibit varying affinities for σ_1R (Matsumoto, 2007; Cobos et al., 2008; Maurice and Su, 2009; Chu and Ruoho, 2016), and appear to share a limited pharmacophore consensus (Walker et al., 1990; Ablordeppey and Glennon, 2007; Newman and Coop, 2007; Weber and Wunsch, 2017). Several candidate endogenous ligands have been proposed over the years, including neurosteroids (Su et al., 1988; Bergeron et al., 1996), sphingosine (Ramachandran et al., 2009) and N,N-dimethyltryptamine (Fontanilla et al., 2009), but these hypotheses have not been conclusively confirmed. Traditionally σ_1R ligands have been classified as agonists or antagonists, depending upon whether they produce or block certain cellular, physiologic or behavioral responses. Although affinities of these ligands for σ_1R have been extensively studied using traditional binding techniques, molecular mechanisms for agonists or antagonists to induce distinct changes of σ_1R remain largely unknown.

The ability to modulate σ_1R function with different ligands has made it an attractive target for developing novel therapeutic strategies. It has been shown that σ_1R agonists have ameliorative effects in several animal models of neurodegenerative disorders, such as Alzheimer's disease (Lahmy et al., 2013; Maurice and Goguadze, 2017; Ryskamp et al., 2019), Parkinson's disease (Francardo et al., 2014), Huntington's disease (Ryskamp et al., 2017), and retinal degeneration (Wang et al., 2016), whereas σ_1R antagonists have pain-relief effects (Merlos et al., 2017). Accumulating evidence also suggest that σRs are critically involved in cellular adaptive mechanisms elicited by psychostimulants (Cai et al., 2017; Katz et al., 2017) and alcohol (Sabino and Cottone, 2017). Therapeutic potentials of σ_1R antagonists have been explored in rodent models of cocaine or methamphetamine addiction (Hiranita et al., 2011; Robson et al., 2014; Sambo et al., 2017).

Whether σ_1R possesses one or two transmembrane domain (TM) has been controversial (Hanner et al., 1996; Aydar et al., 2002; Hayashi and Su, 2007). In recent years atomic force microscopy and solution nuclear magnetic resonance methods were employed to explore σ_1R structures (Carnally et al., 2010; Balasuriya et al., 2012; Ortega-Roldan et al., 2013). Breakthrough on the crystal structures of σ_1R has elucidated its homo-trimer organization, with each protomer containing a single TM and a cytoplasmic ligand-binding pocket (Schmidt et al., 2016). Such structural architecture differs from a dimer-tetramer model postulated by early work (Chu and Ruoho, 2016). Further, crystal structures of σ_1R bound with agonist (+)-pentazocine or antagonist haloperidol showed similar homo-trimer organization, with limited conformational rearrangement (Schmidt et al., 2018), suggesting that trimers may be the lowest free energy state of σ_1R during crystallization. It remains unclear whether ligand binding affects the native high-order organization of σ_1R. This study examined σ_1R oligomerization using molecular, biochemical and pharmacological techniques. The results show that multiple domains on σ_1R coordinate its multimerization. Further, agonists and antagonists dynamically regulate σ_1R oligomerization in distinct manners, and quaternary structures of σ_1R significantly impact ligand binding.

Materials and Methods

Chemicals, radioligands and antibodies. Sources of reagents are as follows: (-)-cocaine HCl, (+)-pentazocine succinate, (+)-SKF 10,047, National Institute on Drug Abuse (NIDA) Drug Supply Program; PRE-084, Tocris (Minneapolis, MN); DTG, BD1008, BD1047, BD1063, NE-100, gifts from Dr. Jonathan L. Katz, CM304, gift from Dr. Christopher R. McCurdy; *d*-erythro-sphingosine, dehydroepiandrosterone, haloperidol, Cayman chemicals (Ann Arbor, MI); BCA protein kit, Pierce (Rockford, IL); PFO, SLS, TCI America (Portland, OR); GDN, Anatrace (Maumee, OH); all other chemicals, Sigma-Aldrich (St. Louis, MO) or Fisher Scientific (Pittsburgh, PA); glutathione-conjugated Sepharose beads, GE Healthcare (Pittsburgh, PA); [^{3}H](+)-Pentazocine (NET-1056, 26.9 Ci/mmol), Perkin Elmer (Boston, MA); anti-Flag rat mAb L5, anti-HA, mAb HA11, anti-Myc mAb 9E10, HRP-conjugated secondary antibodies, Biolegend (San Diego, CA); anti-σ_1R mAb clone B5, Santa Cruz Biotechnology (Santa Cruz, CA).

DNA subcloning and stable expression cell lines. The coding sequences of human σ_1R cDNA were subcloned into CMV promoter-based mammalian expression plasmids expressing N-terminal fusion of HA, Myc or FLAG-2xHis_8 tags (Hong et al., 2017). σ_1R mutants were generated using the QuikChange method, verified by standard DNA sequencing procedures. Plasmids DNA were linearized, transfected into cells using TransIT LT1 reagent (Mirus Bio, Madison, WI) to isolate G418-resistant clones. Alternatively, cells were transiently transfected using PolyJet (SignaGen, Rockville, MD). Cells were then cultured in DMEM with 10% FBS (Sigma), penicillin-streptomycin in humidified incubators with 5% CO_2 at 37°C. G418 (0.5 mg/ml) was included for stable lines, and expression of σ_1R was verified by immunoblot using antibodies against σ_1R or epitope tags.

Rat liver membrane preparations. Fresh liver tissues from mixed gender Sprague-Dawley rats (BioIVT, Hicksville, NY) were rinsed with cold PBS, cut into small pieces with a razor blade, washed with ice-cold sucrose-phosphate buffer (SPB, 0.32 M sucrose, 7.74 mM Na_2HPO_4, 2.26 mM NaH_2PO_4, pH 7.4), and resuspended in SPB (1:10 ratio, w/v in g:ml). Tissues were homogenized in a glass homogenizer with a motor-driven Teflon pestle at 2,000 rpm for 20 strokes, and centrifuged at 1,000 *g* for 10 min at 4°C. The supernatant was centrifuged at 10,000 *g* for 10 min at 4°C. The resulting pellet was resuspended in SPB by vortexing (1:4 w:v), aliquoted, and frozen in liquid N_2.

Drug treatment. Confluent cells in 12-well plates were incubated at 37°C in culture medium with σ_1R ligands for 1 h (Fig. 1A, B, C, Fig. 2A, B), or antagonists for 0.5h, followed by agonist for 1 h (Fig. 1D, E). Cells were then washed with cold PBSCM, harvested and incubated with GDN-Tris lysis buffer (0.1% GDN, NaCl 150 mM, EDTA 1 mM, Tris 10 mM, pH 7.5, and protease inhibitors) for 2 h at 4°C, followed by centrifugation at 20,000 *g* for 20 min. The resulting supernatants were used as GDN lysates. In Fig. 3, GDN lysates of cells were incubated with drugs overnight on ice before gel analysis.

Liver membranes were thawed and divided into equal portions in microfuge tubes. Drugs were added to tubes and incubated at 37°C for 2 h. Tubes were centrifuged at 15,000 *g* for 10 min at 4°C, the pellets were lysed similarly as cells, except the GDN-HEPES lysis buffer used 20 mM HEPES to replace Tris.

Analysis of σ_1R multimeric states by PFO-PAGE and SLS-PAGE. GDN lysates were mixed with an equal volume of 2x sample buffer (40% glycerol, bromophenol blue 0.005%, Tris 100 mM, 8% PFO or 4% SLS, pH 7.5) to a final concentration of 4% PFO or 2% SLS, and heated at 37°C for 10 min. Samples were run in 5-15% polyacrylamide Tris-glycine gels

(running buffer: 0.1% PFO or 0.1% SLS, 25 mM Tris, 192 mM glycine, pH 8.3). Proteins were transferred to PVDF membranes and immunoblotted with Flag, HA or σ_1R antibodies. Chemiluminescent signals were captured with a MultiImage III device (Alpha Innotech, San Leandro, CA) as digital TIFF images without pixel saturation. Integrated densities of bands were quantified using the NIH ImageJ software and normalized to percent of vehicle. The following proteins (from Sigma-Aldrich) were mixed with PFO or SLS sample buffer and used as molecular standards: egg white lysozyme (14 kD), ovalbumin (45 kD), BSA (66 kD monomer, 132 kD dimer), bovine liver catalase (240 kD) and equine apoferritin (443 kD). Due to stable expression of tagged σ_1R, variances of σ_1R levels in cell lysates within each experiment were usually minimal. GDN lysates were also mixed with 4 x SDS sample buffer, heat at 85°C for 10 min, run in SDS-PAGE, transferred and blotted to verify equal loading of total σ_1R.

Crosslinking of σ_1R. GDN-HEPES lysates from cells or rat liver were incubated with 0.2 to 1 mM DSP (a bifunctional, primary amine-reactive crosslinker with a cleavable disulfide bond) at 25°C for 1 h, mixed with SDS sample buffer without DTT, heated at 85°C for 10 min, and run in SDS-PAGE. A parallel set of lysates were treated with DSP, and further incubated with 20 mM TCEP at 25°C for 0.5 h to reduce the disulfide bond in DSP.

[^{3}H](+)-Pentazocine binding in GDN-solubilized cell lysates. Transfected HEK293 cells were harvested from 150 mm dishes, lysed in GDN-Tris buffer at 4°C with gentle shaking, and centrifuged at 20,000 g for 30 min. Supernatants were collected and adjusted to final pH values of approximately 6, 7.5, or 9, by diluting with appropriate combinations of 1 M solutions of Tris-HCl (pH 7.5), Tris base (pH 10.4) or Tris-HCl (pH 4.7) to final 10 mM Tris, and GDN was supplemented to 0.02%. Binding reactions were set up in polystryrene tubes, containing 200 μl diluted lysates and 50 μl drugs (5 nM [^{3}H](+)-pentazocine and various concentrations of

competing ligands). After overnight incubation on ice, 4 ml ice-cold Tris buffer (10 mM, pH 7.5) were added to each tube, and the mixture was rapidly filtrated onto 0.05% polyethylenimine-soaked GF/B filter papers using an M-24 harvester (Brandel Instruments, Gaithersburg, MD), followed by three washes of 3 ml Tris buffer. Dried filters were soaked with 3 ml liquid scintillation cocktail overnight, and measured for radioactivity using a Tri-Carb 2900TR liquid scintillation counter (Perkin-Elmer) at 45% efficiency. Non-specific binding measured in the presence of 10 μM haloperidol was generally <10% of total binding for WT σ_1R, and subtracted from total counts to obtain specific binding. Data were analyzed using GraphPad Prism (San Diego, CA) for non-linear regression to derive B_{max} or K_d values.

Results

Previously we reported a non-denaturing gel method which detected σ_1R monomer, dimer, or high molecular weight (MW) multimers, based on their apparent electrophoretic mobility. The proportion of σ_1R multimers was decreased by the agonist (+)-pentazocine, but increased by the antagonist CM304 (Hong et al., 2017). In this assay, during gel electrophoresis SDS was replaced by perfluorooctanoic acid (PFO), a mild detergent shown to preserve protein oligomers (Ramjeesingh et al., 1999; Penna et al., 2008).

Following literature review σ_1R drugs that are well-characterized as agonists or antagonists were selected for this study. HEK293 cells were stably transfected with the wild-type (WT) human σ_1R containing N-terminal Flag and 2xHis_8 tags (FH-σ_1R, predicted MW of 32 kD: 25 kD σ_1R + 7 kD tags with linker), and cultured to confluency in multi-well plates to minimize samples variability. Cells then were incubated with drugs in culture medium at 37°C for 1 h, washed, and solubilized using a mild detergent glyco-diosgenin (GDN). Lysates were run in PFO-PAGE and immunoblotted with Flag antibodies. The two lower-MW bands matched the estimated size of σ_1R monomer (comprising one σ_1R polypeptide or protomer) and dimer (comprising two protomers). High-MW diffused bands likely represented multiple forms, apparently larger than trimers (three promoters), thus termed as "multimers" in this study. Oligomerization of σ_1R is defined as assembly from monomers to any form containing at least two σ_1R protomers, whereas multimerization specifically refers to formation of σ_1R complexes containing three and more protomers.

σ_1R agonists (+)-pentazocine, 1,3-Di-*o*-tolylguanidine (DTG), (+)-SKF10047, and cocaine all significantly decreased σ_1R multimer band density, with (+)-pentazocine producing largest effect (32 ± 4% of vehicle, Fig. 1A). In contrast, σ_1R antagonists (BD1063, BD1047,

BD1008, and haloperidol) all significantly increased the band density of σ_1R multimers above two-fold of that in vehicle (Fig. 1B), resembling effects of CM304. As they mostly have nanomolar affinities for σ_1R, low micromolar concentrations of these drugs were likely sufficient to permeate through cell membranes and occupy most of intracellular σ_1R sites during incubation, and induce significant effects on its multimerization.

Distinct effects of (+)-pentazocine were dose-dependent, ranging from 0.1 to 2 μM (Fig. 1C). Further, pre-exposure of antagonists (haloperidol, BD1008 or BD1063) in these cells for 0.5 h blocked (+)-pentazocine's effects (Fig. 1D&E). Notably, these drugs did not change the total pool of σ_1R (shown in SDS-PAGE), but altered the proportion of multimers to dimers and monomers. Dose-dependent effects of haloperidol (0.1 to 1 μM) on reversing (+)-pentazocine's effects were also shown in PFO-PAGE (Yano et al., 2018). These data showed that generally σ_1R agonists and antagonists induced opposite effect on σ_1R multimerization. PRE-084 and NE-100 appeared to produce effects as agonist or antagonist, respectively, although not statistically significant.

Other mild detergents were then explored. If lysates were mixed with 2% sodium deoxycholate, only high-MW σ_1R multimeric bands were seen (data not shown). Fortuitously, replacing 4% PFO with 2% sodium lauroyl sarcosinate (SLS) (Reichel, 2012), an ionic detergent less stringent than SDS, yielded remarkable results. σ_1R mainly showed as monomer and multimer bands, with the dimer band largely absent. Consistent with results in PFO-PAGE, (+)-pentazocine decreased, whereas haloperidol increased σ_1R multimers in SLS-PAGE (Fig. 2A). However, this assay had a higher sensitivity. Haloperidol increased σ_1R multimer band densities to approximately four-fold of vehicle, and (+)-pentazocine decreased σ_1R multimer bands to 23 ± 4% of vehicle. Further, in SLS-PAGE significant effects on σ_1R multimeric band densities by

NE-100 (157 ± 19% of control) and PRE-084 (67 ± 7% of control, Fig. 2B) were revealed. Interestingly, σ_1R multimers appeared as multiple high-MW smeared bands, but apparently larger than 100 kD, suggesting that transfected σ_1R might exist in multimeric forms larger than homotrimers.

As most σ_1R is located on intracellular membranes, during incubation drugs permeated through cell membranes to bind σ_1R, and most likely they remained bound to σ_1R during cell lysis, since (+)-pentazocine and haloperidol were shown to dissociate very slowly from σ_1R (dissociation $t_{1/2}$ > 3 h) using traditional radioligand off-rate method (Bowen et al., 1993) or scintillation proximity assay (Schmidt et al., 2018). Further, if lysates from drug-naïve cells were incubated with drugs overnight on ice, similar effects as those in preincubation were seen (Supplemental Fig. 1). Lastly, FH-σ_1R cell lysates exhibited robust binding of [^{3}H](+)-pentazocine (Fig. 7), suggesting that GDN solubilization, to a large extent, preserved active conformations of σ_1R capable of ligand binding.

These features facilitated examination of effects by potential endogenous ligands of σ_1R. Several candidates have been proposed, including progesterone (Su et al., 1988), dehydroepiandrosterone (Bergeron et al., 1996), and *d*-erythro-sphingosine (Ramachandran et al., 2009). Due to their limited water solubility, it was difficult to incubate cells at concentrations close to their binding affinities for σ_1R (high nM to low μM). However, these lipids could be dissolved in ethanol at 10 mM, then mixed with GDN-solubilized FH-σ_1R cell lysates to achieve final concentrations of 10 to 100 μM. Following overnight incubation on ice, lysates were then subjected to SLS-PAGE. Compared with vehicle treatment (0.5% ethanol), progesterone (10 and 50 μM) significantly increased σ_1R multimers (144 ± 19% and 207 ± 26% of vehicle, Fig. 3). Dehydroepiandrosterone and *d*-erythro-sphingosine appeared to induce a slight, dose-dependent

JPET Fast Forward. Published on February 14, 2020 as DOI: 10.1124/jpet.119.262790
This article has not been copyedited and formatted. The final version may differ from this version.

decrease of σ_1R multimers, albeit not statistically significant. Another proposed endogenous ligand for σ_1R, N,N-dimethyltryptamine (Fontanilla et al., 2009), as a Schedule I controlled substance is not available at the current institution and not tested.

In PFO-PAGE and SLS-PAGE, GDN lysates typically were mixed with PFO or SLS and heated at 37°C 10 min before gel analysis. Distinct effects of agonists and antagonists suggest that they differentially affect the stability of σ_1R multimers. To test this idea, GDN lysates from drug-treated FH-σ_1R cells were mixed with PFO or SLS loading buffer, incubated at four different temperatures (25°C, 37°C, 50°C, and 70°C) for 10 min, before analyzed in PFO-PAGE or SLS-PAGE. The proportion of σ_1R multimer was gradually decreased by rising temperatures before disappearing at 70°C. Compare with vehicle, at each condition (+)-pentazocine consistently decreased, whereas haloperidol increased σ_1R multimers (Fig. 4). Even at 50°C, haloperidol clearly protected σ_1R multimers. Hence, the antagonist haloperidol appeared to enhance the thermostability of σ_1R multimers, while agonist (+)-pentazocine had opposite effects.

Several approaches were used to allay the concern that epitope-tagged σ_1Rs in transfected cells may have different quaternary organizations than native σ_1R. First, effects of different epitope tags in stably transfected HEK293 cells were compared. Distinct effects by (+)-pentazocine and BD1008 were preserved for HA-tagged σ_1R (Supplemental Fig. 2A) in PFO-PAGE. Second, HEK293 cells were transiently transfected to express FH-σ_1R at different levels. Regardless of high or low expression, BD1008 increased, whereas (+)-pentazocine decreased FH-σ_1R multimers in SLS-PAGE and PFO-PAGE (Supplemental Fig. 2B).

Further, whether drugs affect endogenous σ_1R multimerization was examined in rat liver tissues, where σ_1R is enriched (McCann and Su, 1991). Rat liver membranes were incubated

with drugs, and solubilized with GDN lysis buffer. Lysates were then subjected to non-denaturing gel analysis, and immunoblot were probed with a mouse monoclonal antibody for σ_1R (clone B5, Santa Cruz Biotechnology). Different from cell lysates, in PFO-PAGE σ_1R were detected as almost exclusively high MW smear bands, very faint signals of dimer bands based on apparent electrophoretic mobility, and no monomers. Compared with vehicle, (+)-pentazocine and BD1008 appeared to increase or decrease the dimer signal respectively (Fig. 5A). In SDS-PAGE σ_1R in rat liver lysates only showed as a single band of 25 kD, if lysates were mixed with SDS (final 1%) and heated to 85°C. If the mixture was incubated at room temperature (RT) for 1 h, a faint band near 75 kD appeared in BD1008-treated samples (Fig. 5B). The apparent MW of this band was consistent with a σ_1R trimer, suggesting that in liver membranes BD1008-induced σ_1R trimers were stable enough to partially resist SDS treatment at RT. Absence of non-specific bands validated this antibody for detecting native σ_1R.

Most importantly, drug effects were convincingly shown when samples were run in SLS-PAGE (Fig. 5C). Compared with vehicle, (+)-pentazocine significantly decreased the proportion of multimers in total σ_1R proteins, with a concomitant increase in σ_1R monomers. In contrast, BD1008 had a significant effect opposite to (+)-pentazocine (Fig. 5C&D). These drug effects were very similar to those seen in transfected HEK293 cells (Fig. 2), but the difference in σ_1R multimer MW was worth noting. In rat liver lysates these bands appeared to range from approximately 70 kD (possible trimer) to beyond 400 kD, with the highest density near approximate 100 kD, but those from cells appeared to have larger MW sizes (Fig. 2). This suggested that high-order quaternary organization of native or heterologously overexpressed σ_1R might not be the same, but drug effects on σ_1R multimerization were preserved overall. It should be cautioned that MW estimation of these bands was limited, due to the nature of these gels.

Crosslinking assays were done to validate the presence of σ_1R multimers. DSP is a bifunctional crosslinker that selectively reacts with primary amines, with a cleavable disulfide bond in its 12Å spacer arm. DSP crosslinking in rat liver GDN lysates induced a 50 kD band after non-reducing SDS-PAGE, which disappeared with TCEP treatment to reduce disulfide-bonds (Supplemental Fig. 3A). Because rat σ_1R has a sole lysine (Lys142) with its side chain solvent accessible, based on human σ_1R crystal structures (Schmidt et al., 2016), the 50 kD band was most likely a dimer formed through crosslinking at Lys142. FH-σ_1R has three more lysine residues in its epitope and linker. DSP crosslinking induced multiple high-MW bands. Beside a clear dimer band, two discernible bands were detected at positions corresponding to trimer and tetramer, and smeared bands above 150 kD (Supplemental Fig. 3B). These data suggested that in transfected cells trimers of σ_1R could exist, yet they might undergo further assembly, thus trimer bands were not detected in non-denaturing gels (Fig.1 & 2).

Recent breakthrough on crystal structures of σ_1R shed new light on key residues mediating homotrimer formation (Schmidt et al., 2016). Mutants of σ_1R at these pivotal positions were examined in non-denaturing gels. In WT σ_1R, the benzyl side chains of Phe191 in three protomers form aromatic interaction with each other (Fig. 6A). Mutation of Phe191 to Gly (F191G) removed this interaction and abolished σ_1R multimerization, but appeared to retain dimerization (lane 1, Fig. 6B). The hydrophobic side chain of Trp136 in WT σ_1R interacts extensive with several residues in the neighboring protomer. Substitution of Trp136 with Gly (W136G) showed severely reduced multimerization, and a dimer but no monomer band (lane 2, Fig. 6B). Crystal structures show that Arg119 and His116 of a WT protomer form a network of hydrogen bonds with Asp195 and Thr198 of its neighboring protomers, which is critical in maintaining trimerization interface. Alanine substitution at either positions (R119A or D195A)

JPET Fast Forward. Published on February 14, 2020 as DOI: 10.1124/jpet.119.262790
This article has not been copyedited and formatted. The final version may differ from this version.

abolished multimerization, but preserved dimerization as observed in PFO-PAGE (lane 6 and 7, Fig. 6B). A σ_1R splice variant skipping exon3 (ΔE3, encoding aa 119 to 149) showed only as dimer but not multimer in PFO-PAGE (lane 3, Fig. 6B), confirming the essential roles of Arg119 and Trp136 in protomer multimerization.

Genetic studies have identified several σ_1R mutants that are implicated in neurodegenerative diseases with motor neuron deficits. The Glu102Gln (E102Q) mutant is associated with juvenile ALS (Al-Saif et al., 2011). In contrast to WT σ_1R, it failed to form multimers, but appeared as dimer exclusively in PFO-PAGE (lane 5, Fig. 6B). The WT σ_1R showed signals of strong monomer, weak multimer, and very faint dimer in SLS-PAGE, but the E102Q mutant and ΔE3 variant exhibited strong dimer signals, suggesting that such sequence alterations abolished σ_1R multimerization, but promoted dimer formation (lane 3 and 5, Fig. 6C). Another disease mutant, Glu138Gln (E138Q) (Gregianin et al., 2016) also appeared to have impaired multimerization (data not shown).

A recent study reported an important role of a GXXXG motif (residues 87-91) in oligomerization of σ_1R. Mutations replacing glycine with residues containing bulky aliphatic side chains appeared to abolish σ_1R multimers but preserve dimers and monomers, as examined in size exclusion chromatography using σ_1R mutants expressed in *E. coli* (Gromek et al., 2014). Two such mutants, Gly91Ile (G91I) and Gly87Leu-Gly88Leu (G87-88L) had low expression levels in transfected cells, as similarly observed in bacterial expression. The G91I mutant showed only as dimer, without multimer or monomer in PFO-PAGE (lane 9, Fig 6B). Weak signals of G87-88L were detected in SLS-PAGE, whereas in PFO-PAGE little if no signals were seen. Overall, these results confirmed the importance of key residues at trimerization interface and the GXXXG motif in σ_1R multimerization.

JPET Fast Forward. Published on February 14, 2020 as DOI: 10.1124/jpet.119.262790
This article has not been copyedited and formatted. The final version may differ from this version.

Further mutational analyses were conducted to explore the dimeric interface. Very weak expression of double mutants (D195A/G91I, D195A/G87-88L, E102Q/G91I, and E102Q/G87-88L) prevented their signal detection in PFO-PAGE, despite faint bands in SLS-PAGE (data not shown). Surprisingly, removing the N-terminal 36 residues (Δ36aa, including the TM region of aa 8 to 32) of σ_1R resulted in a mutant that showed as a distinct monomer in PFO-PAGE and SLS-APGE (lane 11, Fig. 6B&C). The mutant lacking N-terminal 10 residues (Δ10aa) displayed severely impaired oligomerization (lane 16). However, a mutant lacking first 5 residues (Δ5aa) but sparing the TM, retained substantially multimerization (lane 15). Moreover, the E102Q mutant with Δ5aa remained as dimer (lane 14), but was converted to apparent monomer if combined with Δ36aa (land 13). Similarly, Δ36aa deletion also changed dimeric G91I to monomer (lane 12).

These data suggest that in addition to key residues in the trimerization interface and GXXXG motif, the N-terminal (NT) domain of σ_1R play a crucial role in its multimerization by potentially linking two homotrimers to form a hexamer, or multiple homotrimers to high-order oligomers. In fact, the unit cell organization of σ_1R crystals shows a pair of homotrimers linked together through interactions of two parallel NT domains, each from a protomer of the two neighboring homotrimers (Schmidt et al., 2016). Further evidence was obtained in mutational analysis on σ_1R homomeric interaction by co-transfection of Myc-tagged WT σ_1R and a series of deletion mutants of σ_1R with N-terminal glutathione S-transferase (GST) fusion. Even upon gradual truncations of more than 100 residues in the C-terminus of GST-σ_1R, Myc-σ_1R was co-enriched by glutathione beads pull-down. However, this interaction was substantially diminished if the NT of σ_1R was deleted (Supplemental Fig. 4).

JPET Fast Forward. Published on February 14, 2020 as DOI: 10.1124/jpet.119.262790
This article has not been copyedited and formatted. The final version may differ from this version.

Next, the impact of σ_1R oligomerization on ligand binding was studied. GDN-solubilized lysates from FH-σ_1R cells showed robust [^{3}H](+)-pentazocine binding, with a K_d value (37.8 ± 3.3 nM, average ± SEM) in a similar range to that of σ_1R expressed in Sf9 cell membranes (Schmidt et al., 2016), and a B_{max} value (20.3 ± 2.3 pmol/mg protein) several-fold higher than those in native tissues (McCann and Su, 1991; Bowen et al., 1993). Remarkably, σ_1R binding exhibited exquisite sensitivity to pH values in the buffer. Compared with normal buffer of pH 7.5, total binding (in the absence of unlabeled ligands) was markedly enhanced in a basic buffer of pH 9, but reduced in an acidic buffer of pH 6 (Fig. 7A). Kinetic analysis of these homologous competition binding data (Fig. 7B) revealed that in pH 9 there was a significant decrease in K_d value (i.e., increase in affinity) of (+)-pentazocine, rather than an increase in binding B_{max} (Fig. 7C,D). In contrast, acidic buffer (pH 6) significantly decreased not only binding affinity but also B_{max} values of [^{3}H](+)-pentazocine. These changes in ligand binding appeared to correlate with the oligomeric states of σ_1R revealed in PFO-PAGE. Compared with control (pH 7.5), there was a significant increase in σ_1R multimers at pH 9, with a concomitant decrease in dimers and monomers (Fig. 7E). An opposite effect was observed at pH 6. These data suggest that ligand binding to σ_1R is significantly affected by its quaternary structures.

Considering multiple oligomeric states of σ_1R, ideally [^{3}H](+)-pentazocine binding should be analyzed using a multi-state model. However, computer-assisted non-linear regression of binding data showed that a simple, one-site model would suffice (Fig. 7A,B), and Scatchard plot appeared to be linear (Fig. 7A inset). Statistical comparisons of one-site versus two-site models did not consistently yield clear-cut conclusions.

Reduced capacity to bind [^{3}H](+)-pentazocine were observed in GDN lysates of σ_1R mutants deficient in multimerization, including Δ36aa, ΔE3, E102Q, R119A and D195A (Table

1). B_{max} values measured in untransfected HEK293 cells was negligible (2% of WT σ_1R-transfected cells, in pmol/mg protein), presumably due to a low level of endogenous σ_1R. The weak expression levels of these mutants in transfected cells confounded the interpretation of their low B_{max}. For instance, D195A σ_1R still showed approximately 20% of binding B_{max} of WT σ_1R despite its low expression, suggesting that (+)-pentazocine binding was not fully compromised in this dimer-forming mutant. Nevertheless, the monomer-only mutant Δ36aa σ_1R did not bind (+)-pentazocine, despite its sufficient expression. Together with observations that pH-sensitivity of (+)-pentazocine binding correlated with changes of σ_1R multimerization (Fig. 7), these data support the hypothesis that σ_1R multimers exhibit most active conformation for high-affinity (+)-pentazocine binding, whereas its monomers likely do not bind (+)-pentazocine.

Discussion

This study used two non-denaturing gel methods to examine σ_1R oligomerization. In general, agonists decreased σ_1R multimers, whereas antagonists increased multimers (Fig. 1-5). Antagonist binding appeared to stabilize σ_1R multimers, as a higher temperature was required to dissociate σ_1R multimers (Fig. 4).

Although these methods detected multiple high-MW smear bands, they could not determine the stoichiometry of σ_1R multimers. Detergent solubilization might introduce artificial aggregates of σ_1R. However, distinct changes in band signals by ligands argue against this. Further, existence of high-MW σ_1R complex was supported by early purification studies using [^{3}H]azido-DTG or [^{3}H](+)SKF10047 as affinity ligands, in which the labeled protein complex under non-denaturing conditions appeared to be approximately 150 or 450 kD (Kavanaugh et al., 1988; McCann and Su, 1991). In blue native gels, purified σ_1R showed as multiple smear bands from 60 to 480 kD (Schmidt et al., 2016).

In rat liver membranes very little dimer and no monomer of σ_1R were present in PFO-PAGE (Fig. 5A), suggesting that native σ_1R multimeric complex was more resistant to extraction by PFO. Distinct drug effects on σ_1R multimerization were optimally demonstrated by SLS-PAGE (Fig. 5C). σ_1R multimers appeared as high-MW bands including possible trimer, tetramer, and beyond. All σ_1R multimers disappeared in denaturing SDS-PAGE. BD1008 induced a weak band of σ_1R trimer if samples were not heated with SDS (Fig. 5B).

Notwithstanding its limitations, these non-denature gel approaches offered a relatively straightforward readout of σ_1R oligomerization. Results on G91I mutant were consistent between PFO-PAGE (Fig. 6B) and size exclusion chromatography (Gromek et al., 2014). Two recent

studies utilized Förster or bioluminescence resonance energy transfer (FRET or BRET) assays to examine ligand effects on σ_1R oligomerization (Mishra et al., 2015; Yano et al., 2018). These assays are advantageous in monitoring the distance between donor- and acceptor-tagged σ_1R in live cells, while PFO-PAGE and SLS-PAGE appear to be more sensitive in detecting effects by some ligands such as BD1047 and DTG.

To induce maximal effects on σ_1R multimerization, most drugs were used at low micromolar concentrations, approximately 100 to 1000-fold of their K_i values for σ_1R. (+)-Pentazocine showed dose-dependent effects on decreasing σ_1R multimers (Fig. 1C). With a subnanomolar affinity for σ_1R (James et al., 2012), CM304 induced significant effects at 0.1 μM. Although 0.45 μM drugs were sufficient to stabilize oligomers of σ_1R purified from bacteria (Gromek et al., 2014), 100 μM (+)-pentazocine or haloperidol was used in COS-7 cells for FRET analysis (Mishra et al., 2015). Thus, higher concentrations of drugs were necessary to permeate across membranes to bind intracellular σ_1R in cells. Most ligands tested here are relatively selective for σ_1R, but haloperidol also has a high affinity for dopamine D_2 receptors. This action was unlikely involved, because haloperidol had effects on σ_1R multimerization in cold cell lysates (Supplemental Fig. 1).

It is worth noting that effects of PRE-084 and NE-100 on σ_1R multimerization did not correlate with their binding affinities. The binding pocket in σ_1R can accommodate diverse ligands with a charged nitrogen as the central pharmacophore (Ablordeppey and Glennon, 2007). Comparison between σ_1R structures bound with (+)-pentazocine and NE-100 revealed limited conformational rearrangement (Schmidt et al., 2018). These structures likely provided snapshots of σ_1R in its lowest free energy state. However, dynamic conformational changes induced by

different ligands and impact on σ_1R quaternary structures have not been thoroughly examined. Further, drug binding to σ_1R may exhibit different cooperativity. Although (+)-pentazocine fully occupied the binding pocket of each σ_1R protomer in crystal structures, binding kinetic analysis of Flag-tagged σ_1R and molecular dynamics simulation supported a multi-step model of (+)-pentazocine binding (Schmidt et al., 2018). Whether PRE-084 or NE-100 induces different conformational changes or binding cooperativity of σ_1R from (+)-pentazocine will require more sophisticated techniques.

Stabilization of σ_1R multimer by antagonists may be explained by their preferential higher affinity for σ_1R multimers than dimers/monomers. In WT σ_1R haloperidol's IC_{50} value for competing against [^{3}H](+)-pentazocine binding was approximately 1/10 of those in R119A or D195A mutants (data not shown), which forms only dimers and monomers. However, similar K_d values (Table 1) was not sufficient to explain why (+)-pentazocine dissociated σ_1R multimers. Other potential mechanisms, such as negative protomer cooperativity for (+)-pentazocine binding, will be pursued in future studies.

As σ_1R interacts with many protein partners and regulates their function (Schmidt and Kruse, 2019), efficacies of σ_1R drugs in functional assays are likely determined by multiple factors at molecular, cellular, and higher integrative levels. (+)-Pentazocine decreased σ_1R's association with BiP (Hayashi and Su, 2007), whereas haloperidol decreased its association with acid sensing ion channels (Carnally et al., 2010), suggesting that different partners may preferentially interact with specific oligomeric forms of σ_1R. Changes in σ_1R oligomerization by ligands can modulate the availability of σ_1R to associate with its partners, but does not fully account for ligands' efficacies in functional assays.

Data in this study suggest that multiple domains coordinate σ_1R oligomerization. Crystal structures of σ_1R have pinpointed critical residues mediating interactions for homotrimerization (Schmidt et al., 2016). Mutation of Arg119 or Asp195 abolished multimerization in non-denaturing gels, confirming a crucial role of hydrogen bonds at these positions. Further, hydrophobic interactions and van der Waals forces involving Phe191 and Trp136 are also pivotal, as removing their aromatic side chains severely impaired multimerization (Fig. 6B,C). The importance of the GXXXG motif (Gromek et al., 2014) was also substantiated by results of G91I σ_1R in PFO-PAGE. As Gly91 is in close proximity (4-5 Å) to Trp136 of a neighboring protomer in σ_1R crystal structures, mutation to bulky side chain disrupted multimerization.

In non-denaturing gels multiple high-MW smeared bands appeared larger than σ_1R homotrimers, suggesting possible high-order organization of σ_1R trimers. A corollary of this scenario would require additional domains to mediate non-covalent assembly of trimeric building blocks. Current data support the hypothesis that the NT of σ_1R serves such a role. Unlike WT σ_1R and the Δ5aa mutant, Δ10aa and Δ36aa mutants yielded only monomers in PFO-PAGE (Fig. 6B), despite their intact trimerization domains. It is tempting to speculate that intact NT interactions are required to initiate σ_1R high-order assembly.

This provocative hypothesis is partly corroborated by σ_1R crystal structures, in which each unit cell comprises two pairs of homotrimers (Schmidt et al., 2016). Both pairs are linked together through interactions of two parallel NT domains, each from a protomer in the two homotrimers (Fig. 6A). The opposite orientation of the two pairs requires their embedding into two lipid bilayers in native membranes, and is possibly an artifact in crystallization. However, dimerization of homotrimers may resemble a form of native σ_1R oligomerization.

Dimer formation after dissociation of multimers may involve assembly of two protomers from neighboring homotrimers via their NT interactions, or rearrangement of two cognate protomers within a homotrimer. Current results on NT truncations favor the first scenario, but do not rule out the latter. Dimer interactions appeared to be preserved by PFO, but disrupted by the more stringent detergent SLS. Persistence of E102Q or ΔE3 σ_1R dimers in SLS-PAGE is perplexing and requires further investigation. The E102Q mutant was shown to be prone to aggregation and have aberrant cellular location (Wong et al., 2016; Dreser et al., 2017). In co-immunoprecipitation assays, ΔE3 σ_1R exhibited altered association with the dopamine transporter than WT σ_1R (Hong et al., 2017), and exerted dominant-negative effects in disrupting association of WT σ_1R with μ opioid receptors (Pan et al., 2017). These results suggest that dysregulation of σ_1R quaternary structure impairs its physiological function.

Intriguingly, buffer pH significantly altered the oligomeric states of σ_1R (Fig. 7E). Although the underlying mechanism and physiological significance are beyond the scope of this study, a rudimentary inference is that σ_1R multimers dissociate in acidic lysosomes to facilitate degradation. This serendipitous finding helped to examine how σ_1R oligomerization affected ligand binding. Results (Fig. 7) indicated that σ_1R multimers possess high-affinity and high-capacity binding of [^{3}H](+)-pentazocine. Because Δ36aa σ_1R formed monomer exclusively, but lacked binding (Table 1), it was inferred that monomeric σ_1R could not bind (+)-pentazocine. This hypothesis is consistent with a previous study using σ_1R mutants from bacterial expression (Gromek et al, 2014).

In summary, this study demonstrated that multiple domains coordinate the oligomerization of σ_1R. The equilibrium balance between monomers, dimers and multimers of σ_1R is dynamically regulated by agonists or antagonists in distinct manners. Whereas antagonists

JPET Fast Forward. Published on February 14, 2020 as DOI: 10.1124/jpet.119.262790
This article has not been copyedited and formatted. The final version may differ from this version.

promote σ_1R multimerization, agonists facilitate its dissociation (Fig. 8). σ_1R mutants implicated in neurodegenerative diseases displayed aberrant multimerization, suggesting that balance in σ_1R oligomerization is important in its physiological function. Extensive studies have shown that σ_1R associates with a plethora of partner proteins that are involved in diverse cellular signaling pathways. Distinct regulation of σ_1R multimerization by agonists and antagonists may selectively modulate activities of clientele proteins within its interactome network. Future work will shed light on whether σ_1R oligomerization may be precisely controlled by cells' adaptive responses to physiochemical changes in the environment, which in turn may impact on these signaling mechanisms.

Acknowledgments

I thank Drs. Jonathan L. Katz, Mark R. Macbeth, and Jie Jiang for advice and comments on this manuscript, and generous gifts of various σ_1R ligands from Jonathan L. Katz, Christopher R. McCurdy, and NIDA Drug supply program.

Author contributions

Participated in research design: Hong

Conducted experiments: Hong

Performed data analysis: Hong

Wrote the manuscript: Hong

References

Ablordeppey SY and Glennon RA (2007) Pharmacophore models for sigma-1 receptor binding, in *Sigma receptors: chemistry, cell biology and clinical implications* (Matsumoto RR, Bowen WD and Su TP eds) pp 71-98, Springer, New York, NY.

Al-Saif A, Al-Mohanna F and Bohlega S (2011) A mutation in sigma-1 receptor causes juvenile amyotrophic lateral sclerosis. *Ann Neurol* **70**:913-919.

Aydar E, Palmer CP, Klyachko VA and Jackson MB (2002) The sigma receptor as a ligand-regulated auxiliary potassium channel subunit. *Neuron* **34**:399-410.

Balasuriya D, Stewart AP, Crottes D, Borgese F, Soriani O and Edwardson JM (2012) The sigma-1 receptor binds to the Nav1.5 voltage-gated Na+ channel with 4-fold symmetry. *J Biol Chem* **287**:37021-37029.

Bergeron R, de Montigny C and Debonnel G (1996) Potentiation of neuronal NMDA response induced by dehydroepiandrosterone and its suppression by progesterone: effects mediated via sigma receptors. *J Neurosci* **16**:1193-1202.

Bernard-Marissal N, Medard JJ, Azzedine H and Chrast R (2015) Dysfunction in endoplasmic reticulum-mitochondria crosstalk underlies SIGMAR1 loss of function mediated motor neuron degeneration. *Brain* **138**:875-890.

Bowen WD, de Costa BR, Hellwell SB, Walker JM and Rice KC (1993) [3H]-(+)Pentazocine: a potent and highly selective benzomorphan-based probe for sigma-1 receptors. *Molecular Neuropharmacology* **3**:117-126.

Cai Y, Yang L, Niu F, Liao K and Buch S (2017) Role of Sigma-1 Receptor in Cocaine Abuse and Neurodegenerative Disease, in *Sigma Receptors: Their Role in Disease and as Therapeutic Targets* (Smith SB and Su T-P eds) pp 163-175, Springer International Publishing, Cham.

Carnally SM, Johannessen M, Henderson RM, Jackson MB and Edwardson JM (2010) Demonstration of a direct interaction between sigma-1 receptors and acid-sensing ion channels. *Biophys J* **98**:1182-1191.

Chu UB and Ruoho AE (2016) Biochemical Pharmacology of the Sigma-1 Receptor. *Mol Pharmacol* **89**:142-153.

Cobos EJ, Entrena JM, Nieto FR, Cendan CM and Del Pozo E (2008) Pharmacology and therapeutic potential of sigma(1) receptor ligands. *Curr Neuropharmacol* **6**:344-366.

Dreser A, Vollrath JT, Sechi A, Johann S, Roos A, Yamoah A, Katona I, Bohlega S, Wiemuth D, Tian Y, Schmidt A, Vervoorts J, Dohmen M, Beyer C, Anink J, Aronica E, Troost D, Weis J and Goswami A (2017) The ALS-linked E102Q mutation in Sigma receptor-1 leads to ER stress-mediated defects in protein homeostasis and dysregulation of RNA-binding proteins. *Cell Death Differ* **24**:1655-1671.

Fontanilla D, Johannessen M, Hajipour AR, Cozzi NV, Jackson MB and Ruoho AE (2009) The hallucinogen N,N-dimethyltryptamine (DMT) is an endogenous sigma-1 receptor regulator. *Science* **323**:934-937.

Francardo V, Bez F, Wieloch T, Nissbrandt H, Ruscher K and Cenci MA (2014) Pharmacological stimulation of sigma-1 receptors has neurorestorative effects in experimental parkinsonism. *Brain* **137**:1998-2014.

Ganapathy ME, Prasad PD, Huang W, Seth P, Leibach FH and Ganapathy V (1999) Molecular and ligand-binding characterization of the sigma-receptor in the Jurkat human T lymphocyte cell line. *J Pharmacol Exp Ther* **289**:251-260.

Gregianin E, Pallafacchina G, Zanin S, Crippa V, Rusmini P, Poletti A, Fang M, Li Z, Diano L, Petrucci A, Lispi L, Cavallaro T, Fabrizi GM, Muglia M, Boaretto F, Vettori A, Rizzuto R, Mostacciuolo ML and Vazza G (2016) Loss-of-function mutations in the SIGMAR1 gene cause distal hereditary motor neuropathy by impairing ER-mitochondria tethering and Ca2+ signalling. *Human Molecular Genetics* **25**:3741-3753.

Gromek KA, Suchy FP, Meddaugh HR, Wrobel RL, LaPointe LM, Chu UB, Primm JG, Ruoho AE, Senes A and Fox BG (2014) The oligomeric states of the purified sigma-1 receptor are stabilized by ligands. *J Biol Chem* **289**:20333-20344.

Hanner M, Moebius FF, Flandorfer A, Knaus HG, Striessnig J, Kempner E and Glossmann H (1996) Purification, molecular cloning, and expression of the mammalian sigma1-binding site. *Proc Natl Acad Sci U S A* **93**:8072-8077.

Hayashi T and Su TP (2001) Regulating ankyrin dynamics: Roles of sigma-1 receptors. *Proc Natl Acad Sci U S A* **98**:491-496.

Hayashi T and Su TP (2007) Sigma-1 receptor chaperones at the ER-mitochondrion interface regulate Ca(2+) signaling and cell survival. *Cell* **131**:596-610.

Hiranita T, Soto PL, Kohut SJ, Kopajtic T, Cao J, Newman AH, Tanda G and Katz JL (2011) Decreases in cocaine self-administration with dual inhibition of the dopamine transporter and sigma receptors. *J Pharmacol Exp Ther* **339**:662-677.

Hong WC, Yano H, Hiranita T, Chin FT, McCurdy CR, Su TP, Amara SG and Katz JL (2017) The sigma-1 receptor modulates dopamine transporter conformation and cocaine binding and may thereby potentiate cocaine self-administration in rats. *J Biol Chem* **292**:11250-11261.

James ML, Shen B, Zavaleta CL, Nielsen CH, Mesangeau C, Vuppala PK, Chan C, Avery BA, Fishback JA, Matsumoto RR, Gambhir SS, McCurdy CR and Chin FT (2012) New positron emission tomography (PET) radioligand for imaging sigma-1 receptors in living subjects. *J Med Chem* **55**:8272-8282.

Jbilo O, Vidal H, Paul R, De Nys N, Bensaid M, Silve S, Carayon P, Davi D, Galiegue S, Bourrie B, Guillemot JC, Ferrara P, Loison G, Maffrand JP, Le Fur G and Casellas P (1997) Purification and characterization of the human SR 31747A-binding protein. A nuclear membrane protein related to yeast sterol isomerase. *J Biol Chem* **272**:27107-27115.

Katz JL, Hiranita T, Hong WC, Job MO and McCurdy CR (2017) A Role for Sigma Receptors in Stimulant Self-Administration and Addiction. *Handb Exp Pharmacol*.

Kavanaugh MP, Tester BC, Scherz MW, Keana JF and Weber E (1988) Identification of the binding subunit of the sigma-type opiate receptor by photoaffinity labeling with 1-(4-azido-2-methyl[6-3H]phenyl)-3-(2-methyl[4,6-3H]phenyl)guanidine. *Proc Natl Acad Sci U S A* **85**:2844-2848.

Kim FJ, Kovalyshyn I, Burgman M, Neilan C, Chien CC and Pasternak GW (2010) Sigma 1 receptor modulation of G-protein-coupled receptor signaling: potentiation of opioid transduction independent from receptor binding. *Mol Pharmacol* **77**:695-703.

Kourrich S, Hayashi T, Chuang JY, Tsai SY, Su TP and Bonci A (2013) Dynamic interaction between sigma-1 receptor and Kv1.2 shapes neuronal and behavioral responses to cocaine. *Cell* **152**:236-247.

Lahmy V, Meunier J, Malmstrom S, Naert G, Givalois L, Kim SH, Villard V, Vamvakides A and Maurice T (2013) Blockade of Tau hyperphosphorylation and Abeta(1)(-)(4)(2) generation by the aminotetrahydrofuran derivative ANAVEX2-73, a mixed muscarinic

and sigma(1) receptor agonist, in a nontransgenic mouse model of Alzheimer's disease. *Neuropsychopharmacology* **38**:1706-1723.

Li X, Hu Z, Liu L, Xie Y, Zhan Y, Zi X, Wang J, Wu L, Xia K, Tang B and Zhang R (2015) A SIGMAR1 splice-site mutation causes distal hereditary motor neuropathy. *Neurology* **84**:2430-2437.

Martin WR, Eades CG, Thompson JA, Huppler RE and Gilbert PE (1976) The effects of morphine- and nalorphine- like drugs in the nondependent and morphine-dependent chronic spinal dog. *J Pharmacol Exp Ther* **197**:517-532.

Matsumoto RR (2007) Sigma receptors: Historical Perspective and Background, in *Sigma receptors: chemistry, cell biology and clinical implications* (Matsumoto RR, Bowen WD and Su TP eds) pp 1-24, Springer, New York, NY.

Maurice T and Goguadze N (2017) Sigma-1 (sigma1) Receptor in Memory and Neurodegenerative Diseases. *Handb Exp Pharmacol* **244**:81-108.

Maurice T and Su TP (2009) The pharmacology of sigma-1 receptors. *Pharmacol Ther* **124**:195-206.

McCann DJ and Su TP (1991) Solubilization and characterization of haloperidol-sensitive (+)-[3H]SKF-10,047 binding sites (sigma sites) from rat liver membranes. *J Pharmacol Exp Ther* **257**:547-554.

Merlos M, Romero L, Zamanillo D, Plata-Salaman C and Vela JM (2017) Sigma-1 Receptor and Pain. *Handb Exp Pharmacol* **244**:131-161.

Mishra AK, Mavlyutov T, Singh DR, Biener G, Yang J, Oliver JA, Ruoho A and Raicu V (2015) The sigma-1 receptors are present in monomeric and oligomeric forms in living cells in the presence and absence of ligands. *Biochem J* **466**:263-271.

Navarro G, Moreno E, Aymerich M, Marcellino D, McCormick PJ, Mallol J, Cortes A, Casado V, Canela EI, Ortiz J, Fuxe K, Lluis C, Ferre S and Franco R (2010) Direct involvement of sigma-1 receptors in the dopamine D1 receptor-mediated effects of cocaine. *Proc Natl Acad Sci U S A* **107**:18676-18681.

Newman AH and Coop A (2007) Medicinal chemistry: new chemical classes and subtype-selective ligands, in *Sigma receptors: chemistry, cell biology and clinical implications* (Matsumoto RR, Bowen WD and Su TP eds) pp 25-44, Springer, New York, NY.

Ortega-Roldan JL, Ossa F and Schnell JR (2013) Characterization of the human sigma-1 receptor chaperone domain structure and binding immunoglobulin protein (BiP) interactions. *J Biol Chem* **288**:21448-21457.

Pan L, Pasternak DA, Xu J, Xu M, Lu Z, Pasternak GW and Pan YX (2017) Isolation and characterization of alternatively spliced variants of the mouse sigma1 receptor gene, Sigmar1. *PLoS One* **12**:e0174694.

Penna A, Demuro A, Yeromin AV, Zhang SL, Safrina O, Parker I and Cahalan MD (2008) The CRAC channel consists of a tetramer formed by Stim-induced dimerization of Orai dimers. *Nature* **456**:116-120.

Ramachandran S, Chu UB, Mavlyutov TA, Pal A, Pyne S and Ruoho AE (2009) The sigma1 receptor interacts with N-alkyl amines and endogenous sphingolipids. *Eur J Pharmacol* **609**:19-26.

Ramjeesingh M, Huan LJ, Garami E and Bear CE (1999) Novel method for evaluation of the oligomeric structure of membrane proteins. *Biochem J* **342 (Pt 1)**:119-123.

Reichel C (2012) SARCOSYL-PAGE: a new electrophoretic method for the separation and immunological detection of PEGylated proteins. *Methods Mol Biol* **869**:65-79.

Robson MJ, Turner RC, Naser ZJ, McCurdy CR, O'Callaghan JP, Huber JD and Matsumoto RR (2014) SN79, a sigma receptor antagonist, attenuates methamphetamine-induced astrogliosis through a blockade of OSMR/gp130 signaling and STAT3 phosphorylation. *Exp Neurol* **254**:180-189.

Ryskamp D, Wu J, Geva M, Kusko R, Grossman I, Hayden M and Bezprozvanny I (2017) The sigma-1 receptor mediates the beneficial effects of pridopidine in a mouse model of Huntington disease. *Neurobiol Dis* **97**:46-59.

Ryskamp D, Wu L, Wu J, Kim D, Rammes G, Geva M, Hayden M and Bezprozvanny I (2019) Pridopidine stabilizes mushroom spines in mouse models of Alzheimer's disease by acting on the sigma-1 receptor. *Neurobiol Dis* **124**:489-504.

Sabino V and Cottone P (2017) Sigma Receptors and Alcohol Use Disorders. *Handb Exp Pharmacol* **244**:219-236.

Sambo DO, Lin M, Owens A, Lebowitz JJ, Richardson B, Jagnarine DA, Shetty M, Rodriquez M, Alonge T, Ali M, Katz J, Yan L, Febo M, Henry LK, Bruijnzeel AW, Daws L and Khoshbouei H (2017) The sigma-1 receptor modulates methamphetamine dysregulation of dopamine neurotransmission. *Nat Commun* **8**:2228.

Schmidt HR, Betz RM, Dror RO and Kruse AC (2018) Structural basis for sigma1 receptor ligand recognition. *Nat Struct Mol Biol* **25**:981-987.

Schmidt HR and Kruse AC (2019) The Molecular Function of sigma Receptors: Past, Present, and Future. *Trends Pharmacol Sci* **40**:636-654.

Schmidt HR, Zheng S, Gurpinar E, Koehl A, Manglik A and Kruse AC (2016) Crystal structure of the human sigma1 receptor. *Nature* **532**:527-530.

Srivats S, Balasuriya D, Pasche M, Vistal G, Edwardson JM, Taylor CW and Murrell-Lagnado RD (2016) Sigma1 receptors inhibit store-operated Ca2+ entry by attenuating coupling of STIM1 to Orai1. *J Cell Biol* **213**:65-79.

Su TP, London ED and Jaffe JH (1988) Steroid binding at sigma receptors suggests a link between endocrine, nervous, and immune systems [see comments]. *Science* **240**:219-221.

Thomas JD, Longen CG, Oyer HM, Chen N, Maher CM, Salvino JM, Kania B, Anderson KN, Ostrander WF, Knudsen KE and Kim FJ (2017) Sigma1 Targeting to Suppress Aberrant Androgen Receptor Signaling in Prostate Cancer. *Cancer Res* **77**:2439-2452.

Walker JM, Bowen WD, Walker FO, Matsumoto RR, De Costa B and Rice KC (1990) Sigma receptors: biology and function. *Pharmacol Rev* **42**:355-402.

Wang J, Saul A, Roon P and Smith SB (2016) Activation of the molecular chaperone, sigma 1 receptor, preserves cone function in a murine model of inherited retinal degeneration. *Proc Natl Acad Sci U S A* **113**:E3764-3772.

Watanabe S, Ilieva H, Tamada H, Nomura H, Komine O, Endo F, Jin S, Mancias P, Kiyama H and Yamanaka K (2016) Mitochondria-associated membrane collapse is a common pathomechanism in SIGMAR1- and SOD1-linked ALS. *EMBO Mol Med* **8**:1421-1437.

Weber F and Wunsch B (2017) Medicinal Chemistry of sigma1 Receptor Ligands: Pharmacophore Models, Synthesis, Structure Affinity Relationships, and Pharmacological Applications. *Handb Exp Pharmacol* **244**:51-79.

Wong AY, Hristova E, Ahlskog N, Tasse LA, Ngsee JK, Chudalayandi P and Bergeron R (2016) Aberrant Subcellular Dynamics of Sigma-1 Receptor Mutants Underlying Neuromuscular Diseases. *Mol Pharmacol* **90**:238-253.

Wu Z and Bowen WD (2008) Role of sigma-1 receptor C-terminal segment in inositol 1,4,5-trisphosphate receptor activation: constitutive enhancement of calcium signaling in MCF-7 tumor cells. *J Biol Chem* **283**:28198-28215.

Yano H, Bonifazi A, Xu M, Guthrie DA, Schneck SN, Abramyan AM, Fant AD, Hong WC, Newman AH and Shi L (2018) Pharmacological profiling of sigma 1 receptor ligands by novel receptor homomer assays. *Neuropharmacology* **133**:264-275.

Footnotes

This study was supported by Butler University Faculty Startup Fund and Holcomb Research Award (WCH). Portions of the work herein were presented at Experimental Biology (2017, 2019) and Society for Neuroscience (2017) meetings.

Figure legends

Fig. 1 Distinct effects on σ_1R multimerization by agonists or antagonists in PFO-PAGE. HEK293 cells stably transfected with FH-σ_1R were treated with drugs at 37°C (in A, B, and C: agonists or antagonists for 1 h; in D & E: antagonists 0.5 h, then (+)-pentazocine 1 h), lysed in GDN-Tris buffer, and run in PFO-PAGE. A) Agonists decreased high-MW multimers. B) Antagonists increased high-MW multimers. C) Dose-dependent effects by agonist (+)-pentazocine or antagonist CM304. D & E) Interaction of agonist and antagonists on σ_1R multimerization, with representative immunoblots. All panels show column graphs (mean ± SEM) from multiple experiments (n): A, n = 4 – 7; B, n = 4 – 11; C, n = 3 – 6; D, n = 3; E, n = 4 - 7. * $P < 0.05$, ** $P < 0.01$, one-way ANOVA and post-hoc Dunnett's test, compared with vehicle. (+)Pent: (+)-pentazocine; (+)SKF: (+)-SKF10047.

Fig. 2 Distinct effects on σ_1R multimerization by agonists or antagonists, detected with SLS-PAGE which showed a higher sensitivity than PFO-PAGE. A and B) Samples from FH-σ_1R cells pretreated with drugs as in Fig. 1. Representative immunoblots and summary column graphs (mean ± SEM) from multiple experiments: A, n = 3 - 6; B, n = 4 – 8. * $P < 0.05$, ** $P < 0.01$, one-way ANOVA and Fisher's least significant difference test, compared with vehicle. (+)Pent: (+)-pentazocine.

Fig. 3 Effects of putative endogenous ligands on σ_1R multimerization. GDN lysates from drug-naïve FH-σ_1R cells were incubated with ligands on ice overnight, then run in SLS-PAGE. Representative immunoblots and summary (mean ± SEM) from n = 4 – 8 experiments. * $P <$

0.05, ** P < 0.01, one-way ANOVA and Fisher's least significant difference test, compared with vehicle. SPG: *d*-erythro-sphingosine; PROG: progesterone; DHEA: dehydroepiandrosterone.

Fig. 4 (+)-Pentazocine and haloperidol differentially affected the thermostability of σ_1R multimers. FH-σ_1R cells were treated with vehicle or drugs (10 μM) at 37°C for 1 h before lysis. Cell lysates were mixed with 2X concentrated PFO or SLS loading buffer, incubated for 10 min at 25°C, 37°C, 50°C, and 70°C, run in PFO-PAGE or SLS-PAGE, and immunoblotted with Flag antibody. Representative blots from n = 3 experiments. (+)Pent: (+)-pentazocine; Halo: haloperidol.

Fig. 5 Analysis of drugs effects on σ_1R multimerization in rat liver membranes. Rat liver membranes were treated with drugs for 2 h at 37°C, followed by lysis with GDN-HEPES buffer. A) In PFO-PAGE σ_1R predominantly showed as smear bands above approximately 100 kD, while a very weak dimer band appeared to be increased following (+)-pentazocine treatment, and decreased by BD1008. B) In SDS-PAGE only 25 kD σ_1R monomer was present if lysates were heated with SDS. However, σ_1R trimer band (75 kD, ►) was revealed in BD1008-treated samples following RT incubation with SDS. C) Significant effects by (+)-pentazocine and BD1008 in SLS-PAGE. σ_1R multimer bands ranged from approximately 70 kD (possible trimer, ►) to above 300 kD, with most density near 100 kD. D) Summary graph showed σ_1R multimer band densities as % of total σ_1R (mean ± SEM, n = 5 experiments) in SLS-PAGE. ** P < 0.01, one-way ANOVA and post-hoc Dunnett's test.

Fig. 6 Mutational analyses show that multiple domains on σ_1R are critical for its multimerization. A) Structure cartoons of σ_1R with mutated residues annotated. Left: side view of σ_1R homotrimer, with transparent surface presentation and peptide backbone in ribbon. Side chains of specific residues are highlighted. Right: unit cell organization of four σ_1R homotrimers in its crystal structure. Zoomed view: parallel alignment of N-terminal 36 aa from two protomers in neighboring homotrimers. Cartoons are based on PDB code 5HK1 (Schmidt et al., 2016), and generated using UCSF Chimera software. B and C) Distinct electrophoretic migration pattern of σ_1R constructs. GDN lysates from HEK293 cells transiently transfected with WT and mutant FH-σ_1R were run in PFO-PAGE and SLS-PAGE, followed by immunoblot detection using Flag antibodies. Representative blots from n > 3 experiments. Constructs are numbered and aligned in both blots, except lanes 1 and 2 were switched in SLS-PAGE. Lack of signals in lanes 8 and 10 of PFO-PAGE was likely due to low expression of these mutants.

Fig. 7 Correlation of [^{3}H](+)-pentazocine binding with σ_1R quaternary structures in different pH buffers. Lysates from GDN-solubilized FH-σ_1R cells were incubated overnight on ice in Tris buffer of pH 6, 7.5 or 9, and analyzed in binding assays. Representative raw data in A (inset shows Scatchard plot) and binding isotherms in B. Both: duplicate samples (average ± SD). Tot: total binding. C and D) Comparisons of B_{max} and K_d values (mean ± SEM, n = 4 experiments, each with duplicates). E) Modulation of σ_1R oligomerization by buffer pH values, as examined in PFO-PAGE. Top: graph showing σ_1R multimer band densities as % of total σ_1R (mean ± SEM, n = 4 experiments) in PFO-PAGE; bottom, representative blot. * $P < 0.05$, ** $P < 0.01$, one-way ANONA and post hoc Dunnett's test, versus pH 7.5.

Fig. 8 Hypothesis cartoon based on results in this study and previous reports. Agonists and antagonists differentially affect σ_1R multimerization. High-order organization of σ_1R likely comprises multiple (≥2) units of homotrimers. Current data suggest a critical role of the N-terminus in mediating formation of multimers beyond homotrimers.

JPET Fast Forward. Published on February 14, 2020 as DOI: 10.1124/jpet.119.262790
This article has not been copyedited and formatted. The final version may differ from this version.

Table 1. B_{max} and K_d values of [^{3}H](+)-pentazocine binding in HEK293 stably transfected with σ_1R constructs. B_{max} values were adjusted to total protein concentrations in lysates. Shown values are mean ± SEM from n = 3 experiments, each with duplicates, except WT (n = 4), E102Q and ΔE3 (n = 2). B_{max} of endogenous σ_1R in untransfected HEK293 cells was 2% of that in WT transfected cells, and was subtracted from these values. Note small B_{max} values of mutants except Δ36aa were partly attributed to their lower expression levels than WT (Fig. 6). All had N-Myc tag except FH-σ_1R Δ36aa.

	σ_1R					
	WT	**Δ36aa**	**R119A**	**D195A**	**E102Q**	**ΔE3**
B_{max} (pmol/mg protein)	16.6 ±3.5	0.08 ±0.05	1.83 ±0.13	3.67 ±0.26	0.99 ±0.06	0.21 ±0.22
K_d (nM)	16.4 ±7.5	14.0 ±3.2	9.8 ±1.4	12.9 ±2.7	5.0 ±0.6	17.0 ±14.1

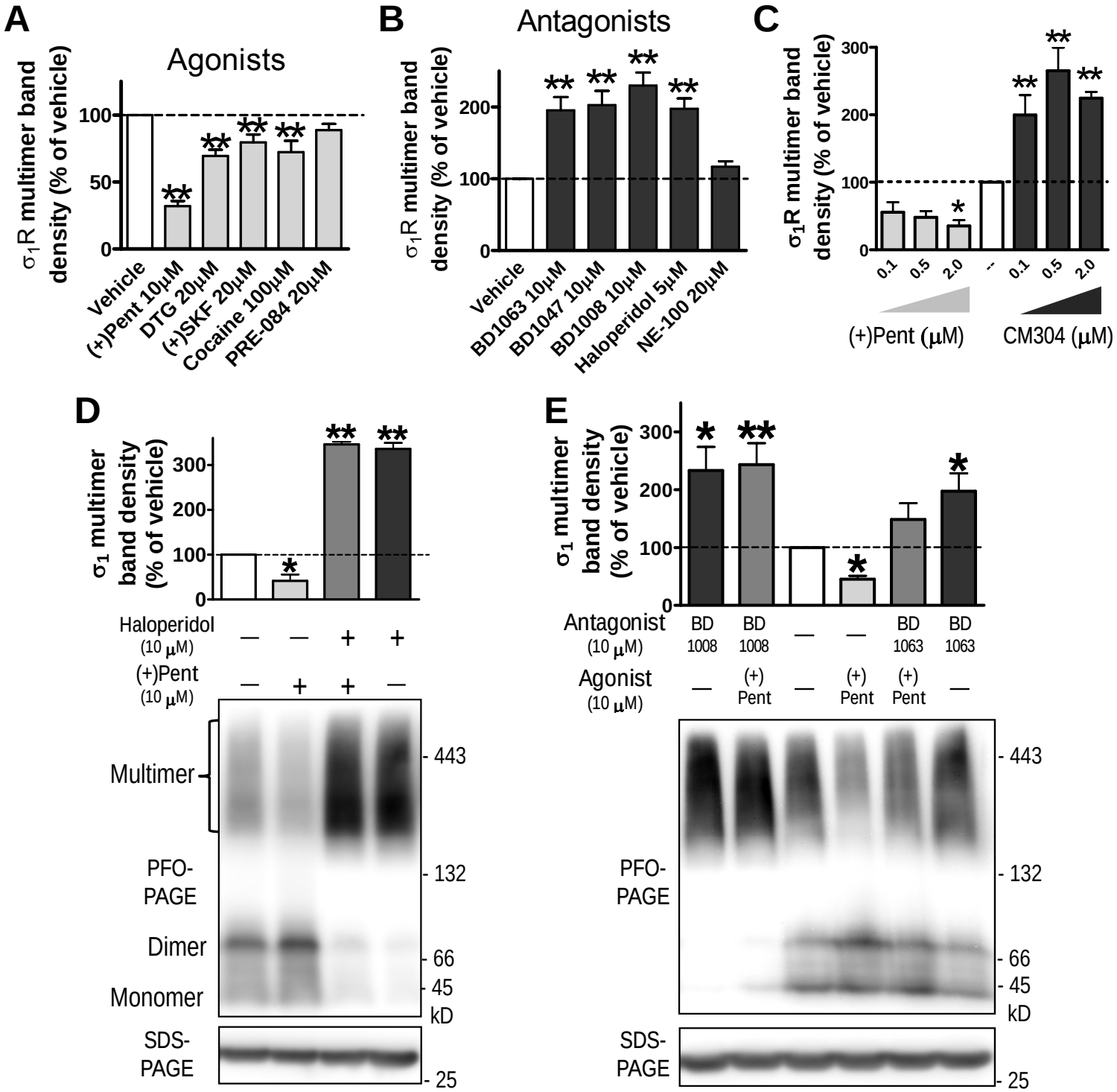

Figure 2

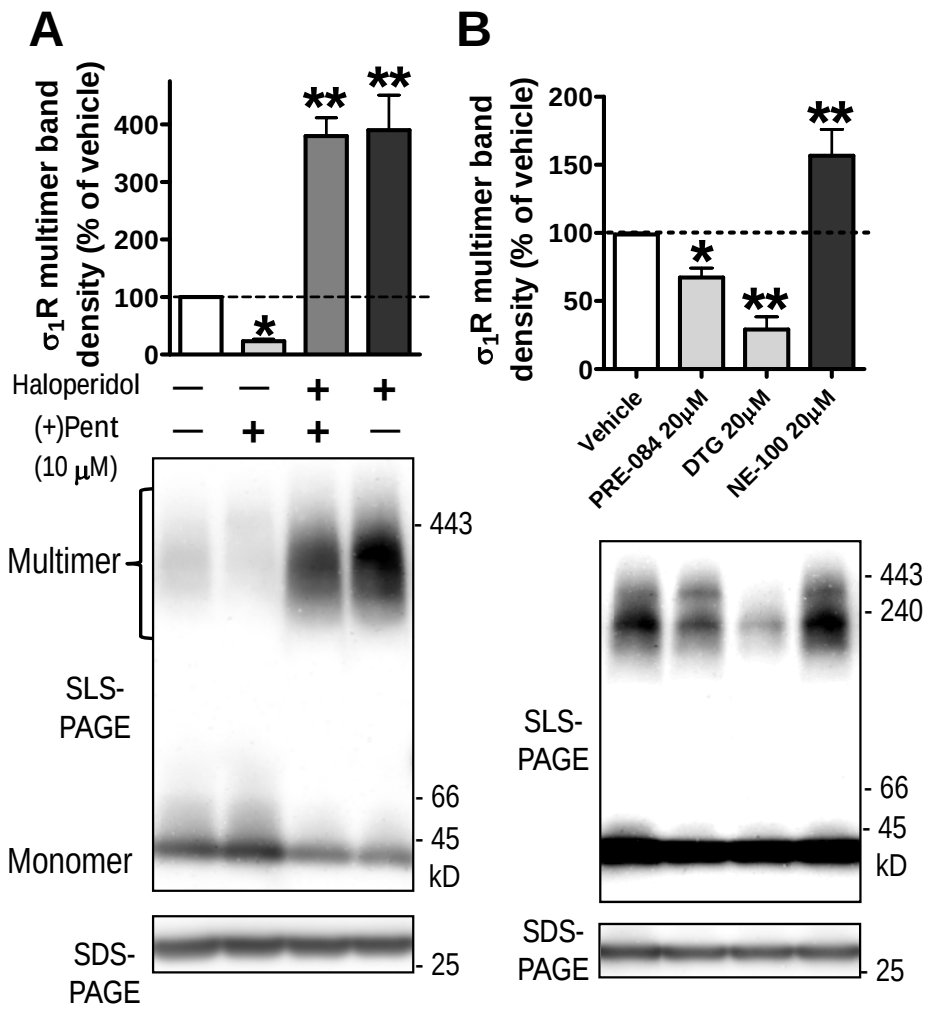

Figure 3

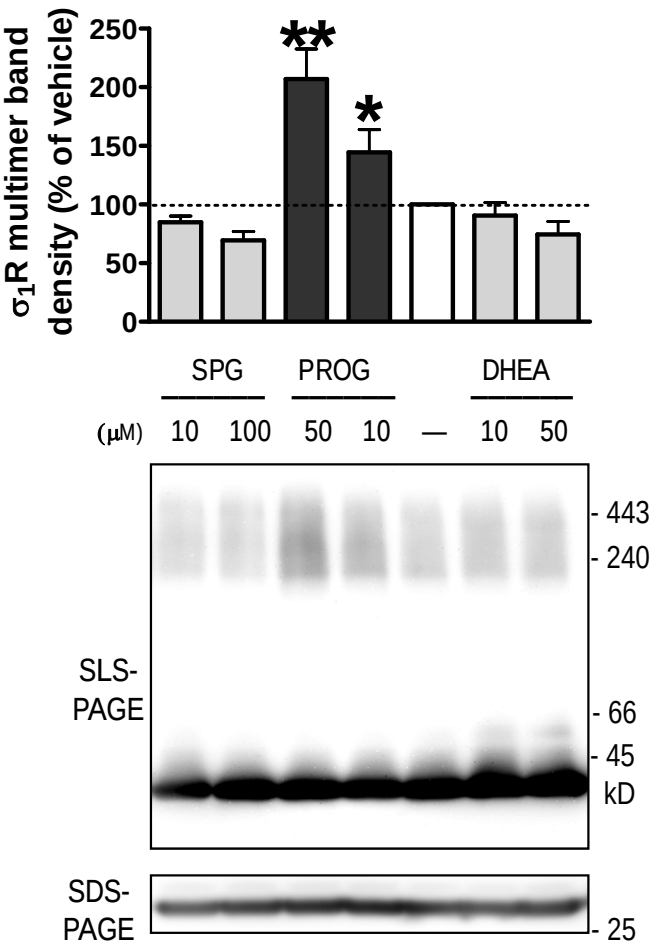

JPET Fast Forward. Published on February 14, 2020 as DOI: 10.1124/jpet.119.262790
This article has not been copyedited and formatted. The final version may differ from this version.

Figure 4

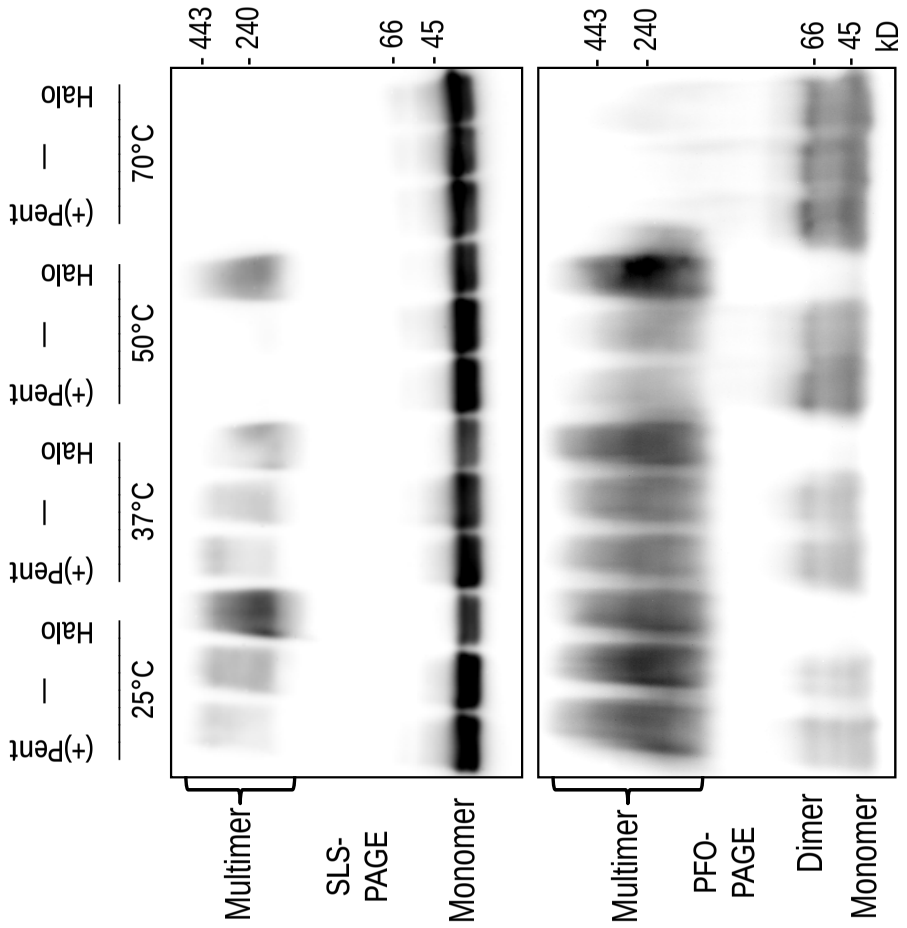

Figure 5

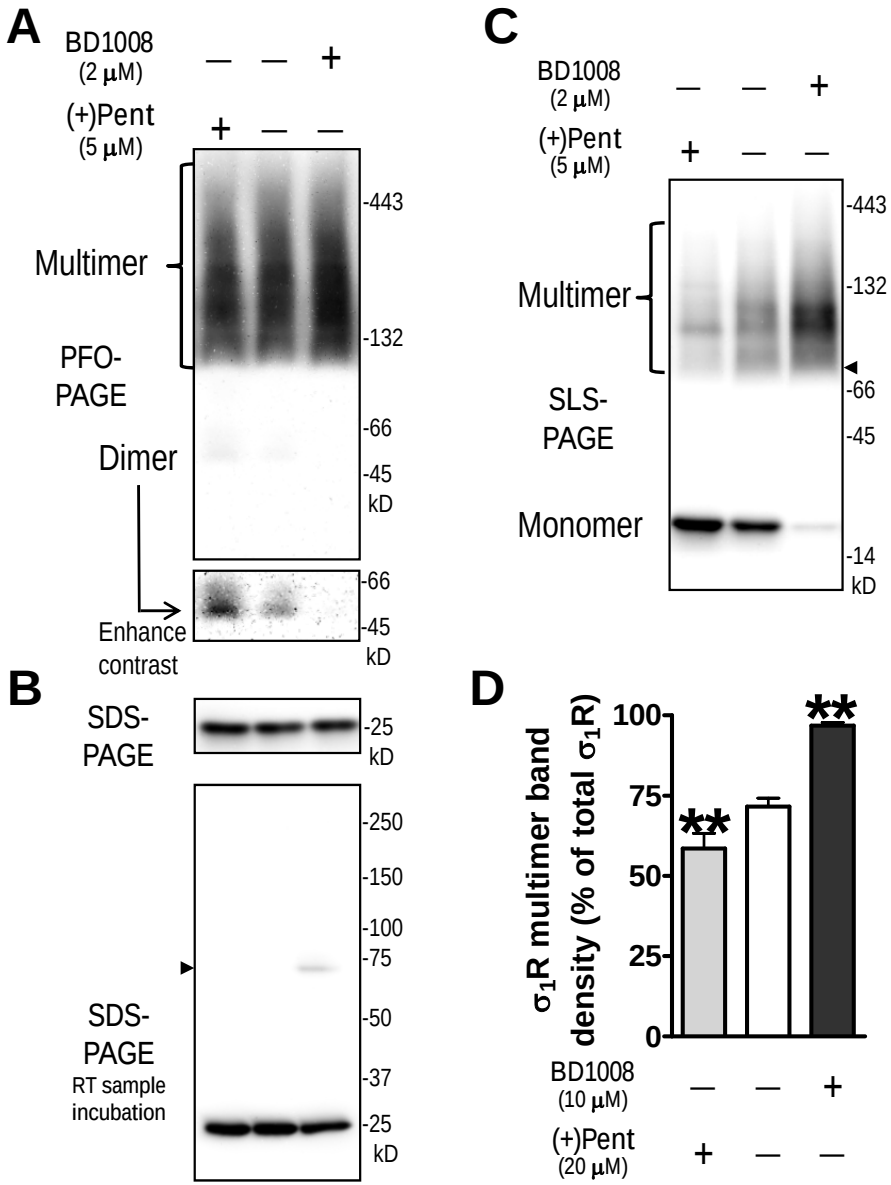

JPET Fast Forward. Published on February 14, 2020 as DOI: 10.1124/jpet.119.262790
This article has not been copyedited and formatted. The final version may differ from this version.

Figure 6

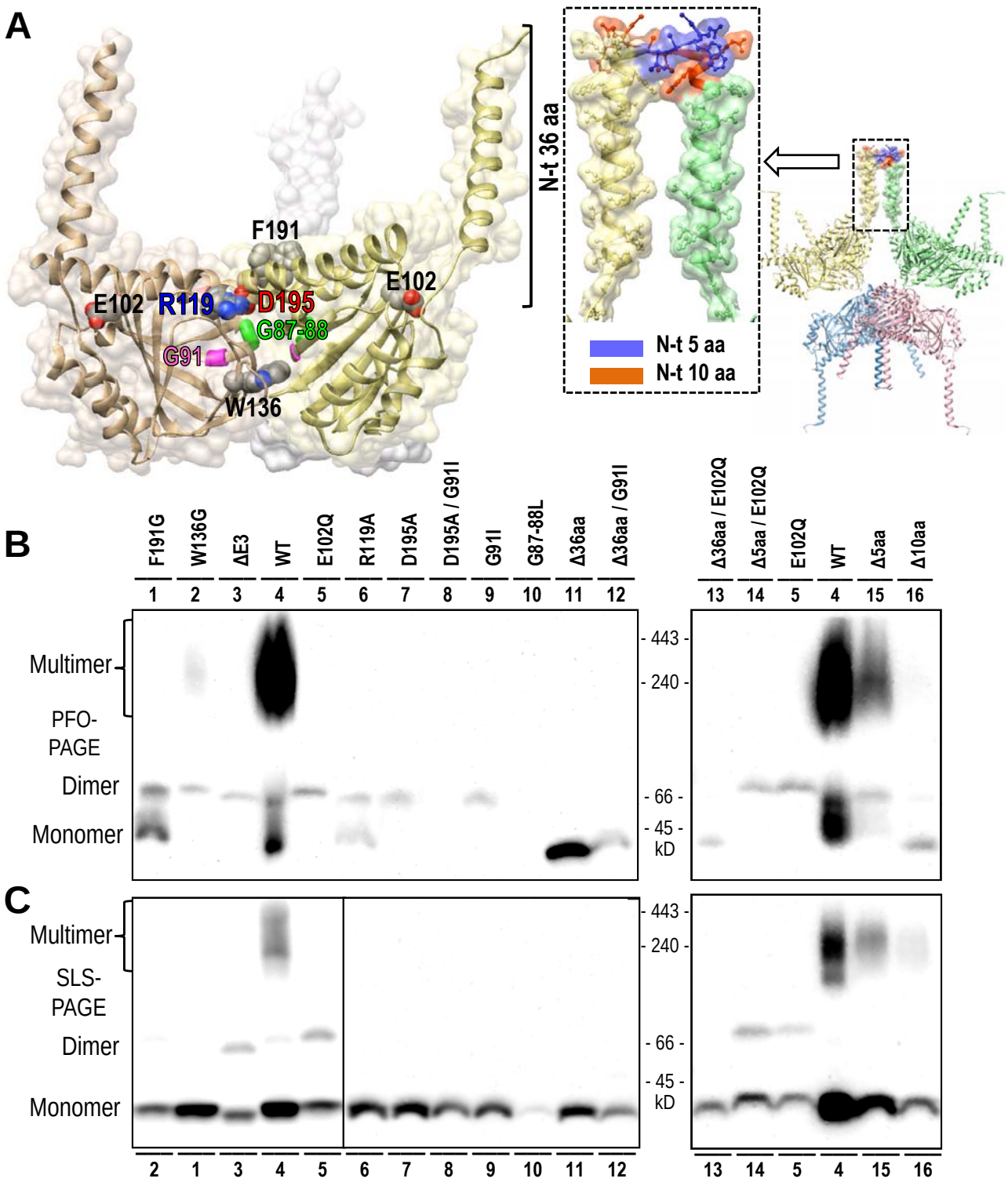

Figure 7

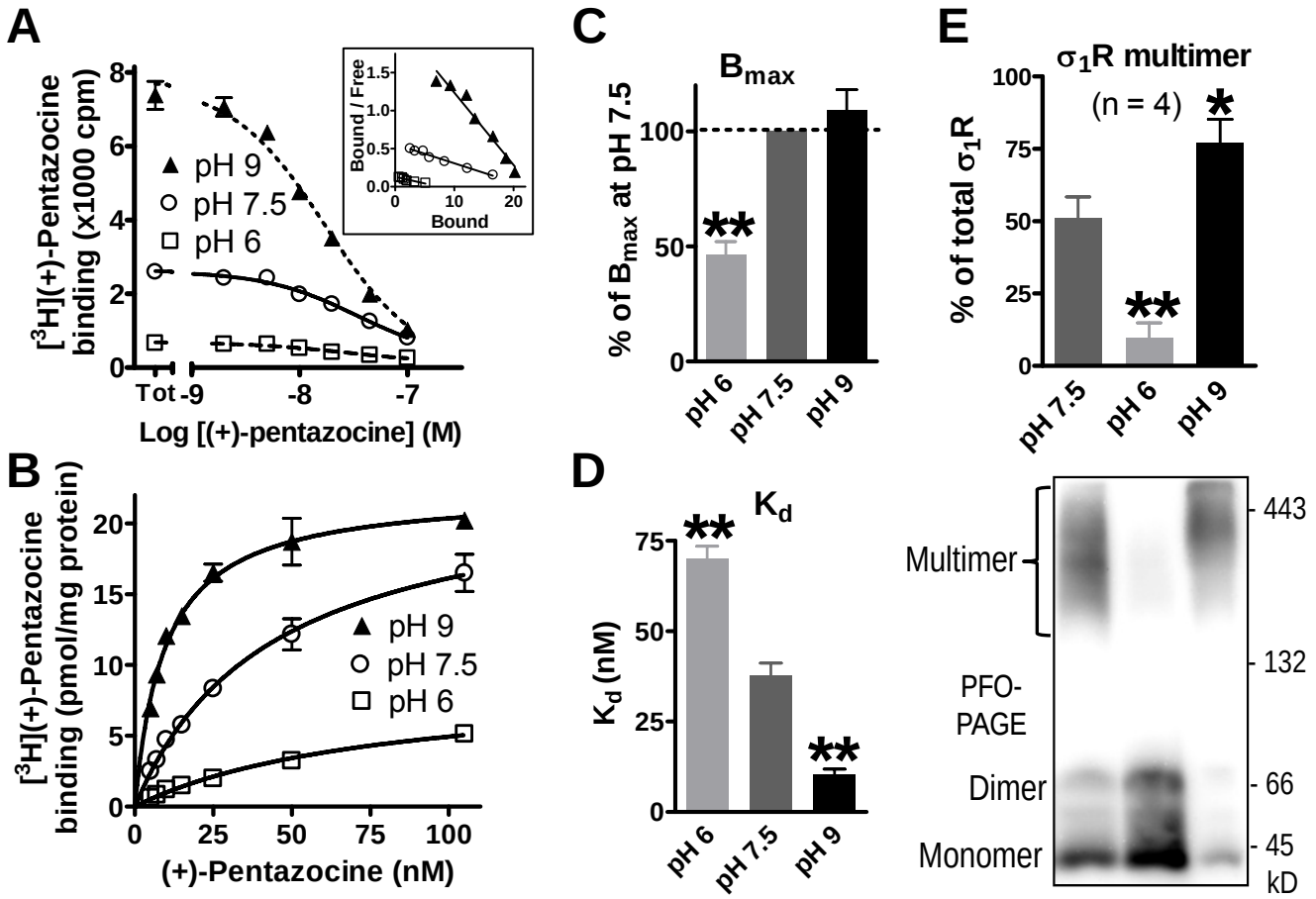

Figure 8